Nuclear Inst. and Methods in Physics Research, A 1052 (2023) 168257

Contents lists available at ScienceDirect

Nuclear Inst. and Methods in Physics Research, A

journal homepage: www.elsevier.com/locate/nima

Full Length Article

The XYU-GEM: Ambiguity-free coordinate readout of the Gas Electron Multiplier

K.J. Flöthner [a,b,*], D. Janssens [a,c,d,**], F. Brunbauer [a], S. Ferry [a], B. Ketzer [b], M. Lisowska [a,e], H. Muller [a,f], R. de Oliveira [a], E. Oliveri [a], G. Orlandini [a,g], D. Pfeiffer [a,h,i], J. Samarati [a,h], L. Ropelewski [a], F. Sauli [a], L. Scharenberg [a,f], M. van Stenis [a], A. Utrobicic [a,j], R. Veenhof [a]

[a] European Organization for Nuclear Research (CERN), 1211 Geneva 23, Switzerland
[b] Helmholtz-Institut für Strahlen- und Kernphysik, University of Bonn, Nußallee 14–16, 53115 Bonn, Germany
[c] Inter-University Institute for High Energies (IIHE), Belgium
[d] Vrije Universiteit Brussel, 1050 Brussels, Belgium
[e] Université Paris-Saclay, F-91191 Gif-sur-Yvette, France
[f] Physikalisches Institut, University of Bonn, Nußallee 12, 53115 Bonn, Germany
[g] Friedrich-Alexander-Universität Erlangen-Nürnberg, Schloßplatz 4, 91054 Erlangen, Germany
[h] European Spallation Source ERIC (ESS), Box 176, SE-221 00, Lund, Sweden
[i] University of Milano-Bicocca, Department of Physics, Piazza della Scienza 3, 20126 Milan, Italy
[j] Ruder Bošković Institute Bijenička c. 54, 10000 Zagreb, Croatia

ARTICLE INFO

Keywords:
Gas Electron Multiplier (GEMs)
Micropattern gaseous detectors
Position reconstruction
Spatial resolution

ABSTRACT

We describe the development of a position-sensitive Gas Electron Multiplier detector prototype, providing for each ionizing event three coordinates: the cartesian X and Y, and U at 45°. Simultaneous recording of the three projections permits ambiguity-free reconstruction of multiple tracks, and aims at operation in very high intensity radiation fields.

1. Introduction

The Gas Electron Multiplier (GEM) [1] is a high gain gaseous detector capable of detecting ionizing events at radiation fluxes up to, and above, 10^6 mm^{-2} s^{-1} [2]. Sub-mm position determination is achieved by collecting the amplified electron charge on sets of narrow-pitch anode strips, and performing a center-of-gravity calculation on the recorded charge distributions. Two-dimensional localization is performed by sharing the charge on two perpendicular sets of strips, named X and Y [3]. The projective coordinate readout scheme has been adopted for most GEM-based experimental setups; a comprehensive summary of which can be found in [4].

For large detection areas and high-rates events can overlap in time, resulting in ambiguities in the position determination. In the case of charged particle trackers, this can be resolved by combining the information from several aligned detectors, often mounted at different angles. This is not always possible, with neutral radiation or single photon detection, like the COMPASS RICH detectors [5], being prime examples. One can make use of the redundant 1D XYU strips instead of 2D pads, reducing required channels and improving resolution.

Various methods have been used to permit operation in high-rate environments. In the central region of the upgraded GEM-based tracker of the COMPASS spectrometer, the strip readout is replaced by a matrix of small pads equipped with individual charge readout due to its location at the highest beam flux [6]. While effective for ambiguity-free reconstruction of multiple events, this method vastly increases the electronics inventory and lessens the position accuracy. In an alternative scheme, the so-called hexaboard, the anode consists of an array of hexagonal pads interconnected on the back plane along three sets of readout strips at 60° to each other [7]. Permitting to reconstruct multiple events a few mm apart [8], the difficulty in manufacturing reliable multi-layer printed circuit boards with thousands of metallized holes has discouraged the adoption of this scheme for large size detectors. Alternative methods to implement three-projections readout were developed for the resistive MICROMEGAS with capacitive coupling; however, this method is limited to moderate particle rates [9].

Motivated by the increasingly demanding requirements of particle physics experiments at high luminosity colliders, Fabio Sauli conceptualized a simpler readout scheme providing three projective coordinates for each detected event, named the XYU-GEM. Its development will

* Corresponding author at: European Organization for Nuclear Research (CERN), 1211 Geneva 23, Switzerland.
** Corresponding author at: European Organization for Nuclear Research (CERN), 1211 Geneva 23, Switzerland.
E-mail addresses: karl.jonathan.floethner@cern.ch (K.J. Flöthner), djunes.janssens@cern.ch (D. Janssens).

https://doi.org/10.1016/j.nima.2023.168257
Received 10 October 2022; Received in revised form 30 March 2023; Accepted 31 March 2023
Available online 1 April 2023

Table 1
Optimized design and practical manufactured geometry.

	Optimized			Manufactured		
Strips	X	Y	U	X	Y	U
Pitch (μm)	400	400	400	400	400	283
Width (μm)	50	150	350	80	180	220
Insulator		25			12.5	
Thickness (μm)			12.5			22.5

be presented here. While the optimal choice would be for the three coordinates to be at 60° to each other, the first prototype, based on existing mechanical structures, had two perpendicular sets of readout strips (X and Y) and one at 45° to the others (U).

Alongside the additional information gained from adding the bottom coordinate layer for ambiguity resolution or spatial resolution improvement, one can envision other applications, such as using the U strips solely for triggering. In this configuration, the geometry of the third layer would be coarse and not necessarily confined to strips alone.

2. Anode readout circuit design and manufacturing

Based on a standard Triple-GEM design[1] [10], the detector has been modified to avoid the need for assembly bolts through the signal strip layers and to mount three GEM foils, a cathode and an anode plane in a gas-tight box. The operating conditions were the standard used for the COMPASS tracker with a gas mixture of argon and CO_2 70–30. The high-voltage is distributed to all electrodes through a resistor chain[2] identical to the one given in [10], as visible in Fig. 1. With an active area of 10×10 cm^2, the detector has 256 readout strips with a 400 μm pitch both for X and Y (identical pitch as in [10]), and 511 strips at 283 μm pitch for U. The latter ensures a discrete symmetry every 400 μm in the x- and y-direction, with a diagonal strip running through the vacant space of the upper two layers (see Fig. 2).

A chain of simulation programs (Garfield++ [11] and COMSOL Multiphysics [12]) has been used to estimate the optimum geometry that provides near-equal collected charge for the three sets of readout strips that are separated by thin insulating ridges. The optimized parameters can be found alongside the ones used for production in Table 1. Here the optimized width of the X and Y strips to ensure equal sharing would be 50 and 150 μm, respectively. However, with the present manufacturing procedure, it was found that too fine strips would tend to detach from the insulator during the Kapton etching process. As a result, their widths were increased to 80 and 180 μm, resulting in a non-equal charge sharing. Better control over the manufacturing may allow the following devices to approach the optimum layout.

Fig. 3 shows the result of the charge sharing calculation for the optimized and manufactured design; experimental measurements confirm the unbalance of the collected charge (see later).

The XYU readout board manufacturing process, developed by CERN's Micro Pattern Technology (MPT) group, aimed to realize three overlapping sets of metallic strips at different angles, separated by thin insulating ridges. For the upper two layers, the insulating material between the neighboring strips in the same coordinate plane has been removed, exposing the copper strips of the layer below. This ensures direct collection of the shared electron charge on the three electrodes (see inset in Fig. 2). This structure differs from those used in other devices, e.g., the resistive MICROMEGAS that achieves two-dimensional readout by utilizing capacitive couplings through the insulators, which could charge up and affect the high-rate performances [13].

[1] The gap sizes are 3, 2, 2, and 2 mm for the drift gap, first transfer region, second transfer region, and induction gap, respectively.

[2] $E_{\mathrm{Drift}}/E_{\mathrm{T1,T2,Induction}}/E_{\mathrm{GEM1}}/E_{\mathrm{GEM2}}/E_{\mathrm{GEM3}} = 2.45/3.67/80.7/73.4/64.6$ kV/cm.

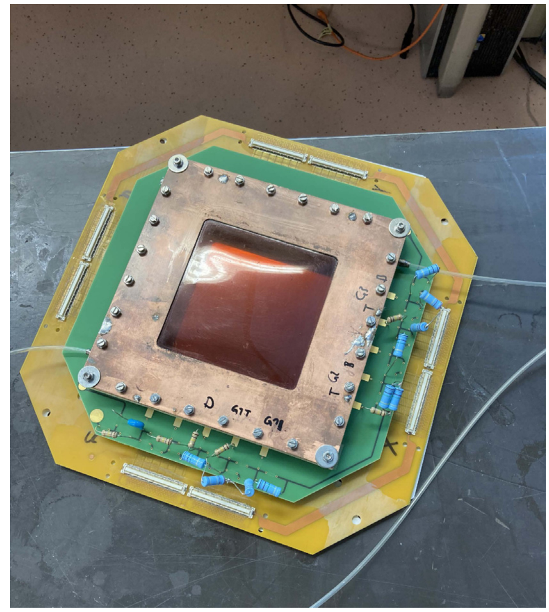

Fig. 1. Prototype of the XYU-GEM detector.

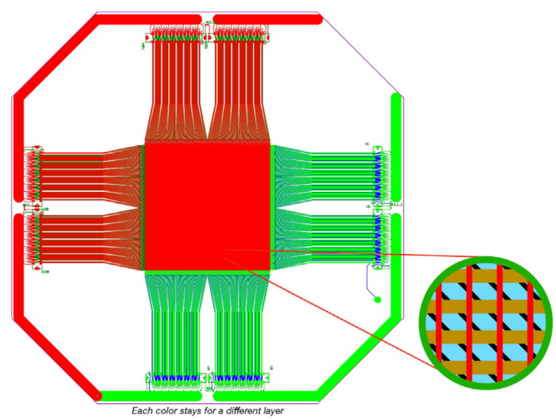

Fig. 2. Schematics of the XYU anode readout board.

Fabrication of the board required several processing steps, here only briefly described. First, the bottom layer (U) is photolithographically patterned on a single-side copper-clad 12.5 μm polyimide foil; the layer is laminated on a 1.6 mm thick fiberglass plate, that will constitute the main supporting board. The middle layer (Y) is then patterned on the bottom side of a double-side copper-clad thin polyimide foil and coated with an etchable glue 10 μm thick; the U and Y layers are pasted together under pressure. To allow the realization of the metalized holes contacts for the connector, the copper layer thickness for the X strips was increased to 15 μm; calculation shows that this increase over the 5 μm design value only slightly affects the sharing. With one more photolithography step, the top copper layer is patterned to realize the X strips. The composite structure then undergoes several stages of polymer and glue etching to open the channels for charge collection on the three layers of metal strips. Fig. 4 is a magnified view of the overlapping strips, and a schematic cross-section of the structure.

Before assembly into the detector, the readout board undergoes a set of electrical testing procedures to verify connectivity and the absence of shorts between strips.

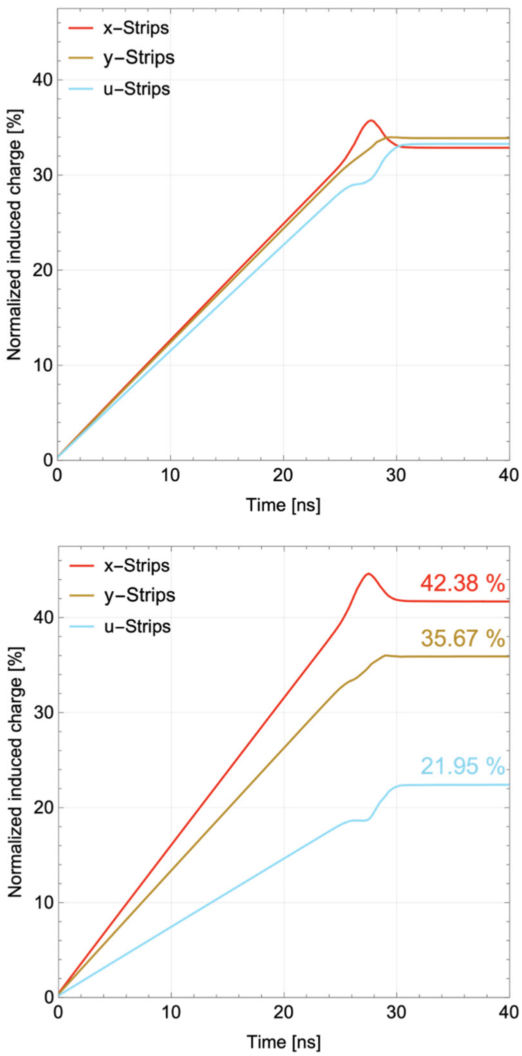

Fig. 3. Computed collected charge as a function of time for the optimized (top) and actually manufactured (bottom) XYU readout geometry.

3. Experimental measurements

For the measurements in the laboratory the detector was equipped with a strip readout electronics based on the ATLAS/BNL 64-channels VMM3a chip with a peaking time set at 200 ns, and the RD51 Scalable Readout System (SRS) for digitizing the input charge of all strips [14]. For confirmation, the signal current from different layers was measured with pico-amperometers while the bottom side of the last GEM was read out with a Multichannel Analyzer. To irradiate the detector, we used 5.9 keV X-rays from an uncollimated ^{55}Fe source that, unless stated otherwise, was placed at a sufficient distance to cover the full active area during the measurements. For what follows, a detector gain of the order of 10^4 was used.

As expected, the detector built with the geometry in Table 1 exhibits an unequal charge sharing between coordinate planes, due to the manufacturing constraints discussed. Fig. 5 shows the pulse height spectra recorded on the three projections on exposure to a 5.9 keV ^{55}Fe X-ray source; the relative ratios between the main peaks are 42: 38: 20, a sharing confirmed by a direct measurement of currents on the three coordinates (45: 34: 21), corresponding well to the simulations done using the actual production parameters.

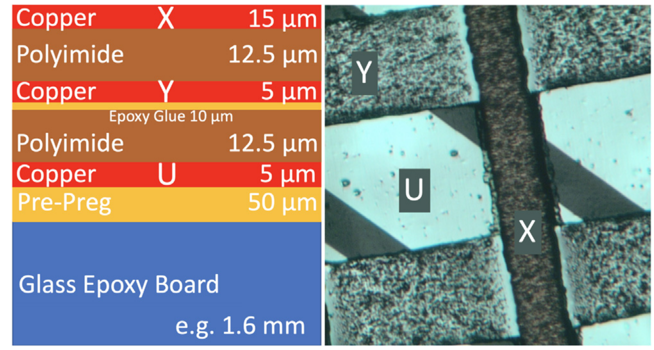

Fig. 4. Schematic cross section and close view of the three overlapping strips.

Using the ^{55}Fe source, the chamber was irradiated to study the charge correlation between the coordinates. Fig. 6 shows a good correlation between the charges on X and Y and, respectively, on X and U coordinates. As indicated above, the charge on U is lower by about a factor of two due to the detector manufacturing parameters.

The charge sharing ratios, imposed by the manufacturing technology, can be modified by applying small polarization voltages to the anode strips; with +15 V on the U strips, the charge on the three coordinates is almost equal. The present design of the front-end electronics does not allow the application of a voltage at the input of the DC-coupled amplifiers; this feature could be implemented with a circuit modification or by using an adaptor.

For each event contained in the main 5.9 keV peak, the cluster size has been deduced from the root mean square (RMS) of the number of adjacent channels going over the threshold. After considering the pitch of the strips (400, 400 and 283 μm respectively, for the X, Y and U coordinates), the cluster size is shown in Fig. 7 for each coordinate plane. As expected, due to their smaller total amount of collected charge, the U distribution is slightly narrower; this difference is not expected to affect the localization properties of the detector significantly. The average value for X and Y, around 375 μm, is consistent with previously measured values in GEM detectors with standard XY projective strip readouts [10]. While the results of the three coordinates are encouragingly close, there is an apparent discrepancy looking at the cluster size of U. This warrants further investigation.

Since, by design, the readout system is inherently overdetermined, the U coordinate of an event within the photopeak can be deduced

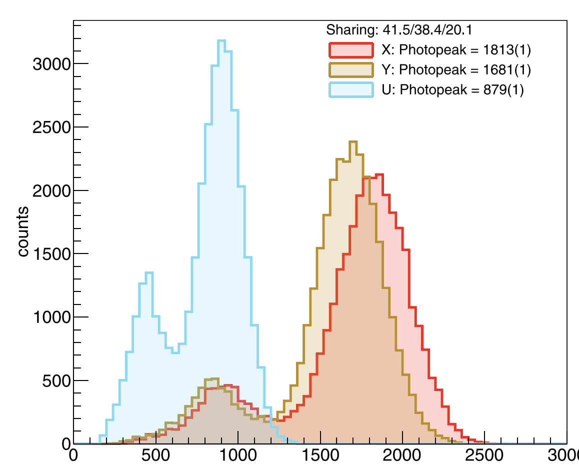

Fig. 5. Pulse height spectra recorded for 5.9 keV X-rays on the X, Y and U projections.

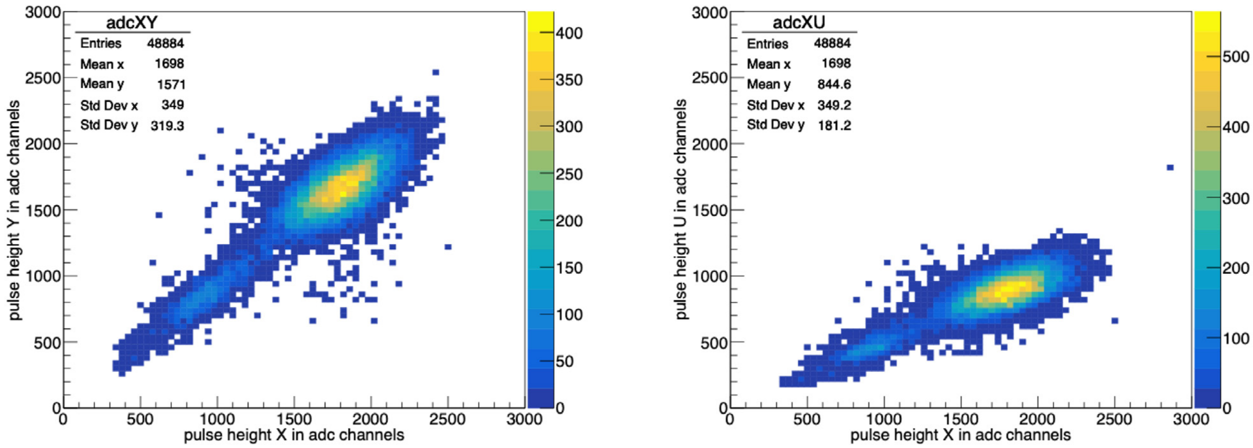

Fig. 6. Recorded charge correlation between XY (left) and XU (right) coordinates.

using the X and Y projections. We analyzed the residual distribution of the difference between the reconstructed, $U(X,Y)$, and measured position in U. This revealed a small distortion of the correlations, probably due to the angle of the U strips slightly deviating from 45°. After correcting for this, the result of the calculation is shown in Fig. 8. A Gaussian fit of the distribution has a FWHM of 127 μm. To improve the event selection, by reducing the uncorrelated noise hits in the U and XY-readout, only events in this distribution that deviate at most a distance less than a few times the strip pitch form zero are accepted.

The multi-track capability of the detector could not be verified in the laboratory, due to the low intensity of the source; we have therefore emulated a multi-particle event, adding up by software several recorded single-particle events into a single frame. Fig. 9 is an example of nine events overlapping, with the X,Y and U recorded strips and a circle marking their known positions. Due to the large number of strips with signals, the frame shows also several accidental three-strips crossings. Despite falling short of a proof of its capacity to disentangle multi-particle events, it showcases its potential given the additional information available from the inclusion of the third coordinate layer.

Due to charging-up of the insulator in the holes, the effective gain of the detector after powering changes under irradiation, reaching a

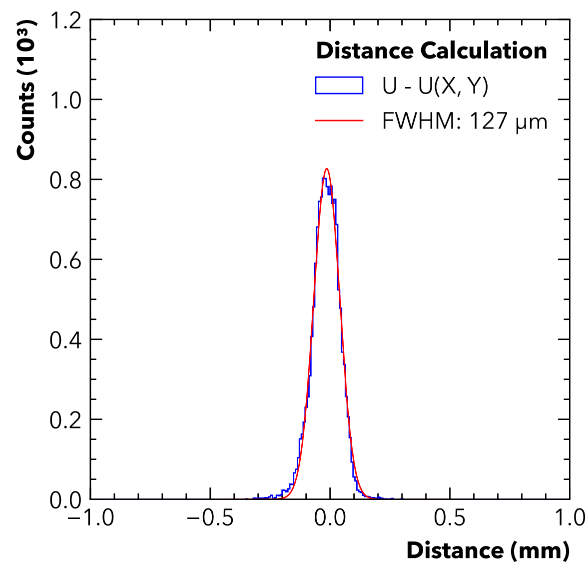

Fig. 8. Computed distance of the U projection from the hits position obtained from the X and Y coordinates, using $U(X,Y) = 511 - X - Y$, where 511 is the total number of U strips.

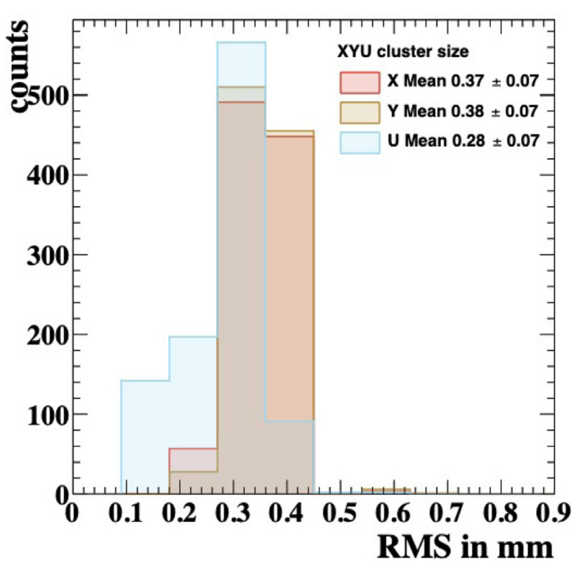

Fig. 7. Cluster sizes RMS for X, Y and U.

constant value within a time that depends on source intensity; the hole's geometry affects the amount and sign of the change [2]. It was observed that the relative charge sharing between the three coordinates changes by about 10% during irradiation, possibly due to a modification of the field lines structure resulting from the accumulation of electrons on the insulator's ridges separating the coordinate layers.

An example of change of sharing with time, after normalization to the gain as measured on the bottom electrode of the last GEM, and recorded at a moderate source intensity (∼2.5 Hz mm^{-2}) is seen in Fig. 10; the sum of the charges is constant, showing that there are no losses. In addition, we measured the saturated sharing for rates up to ∼60 kHz cm^{-2}, which only showed minimal variation. The extent of the change (a few percent) is not expected to affect the detector's performances.

4. Summary and future work

The present work demonstrates the capability of the XYU-GEM structure to detect and localize radiation, providing three independent projections of the events. To assess the properties and efficiency of multi-hit events, it is planned to expose the detector to a high-intensity

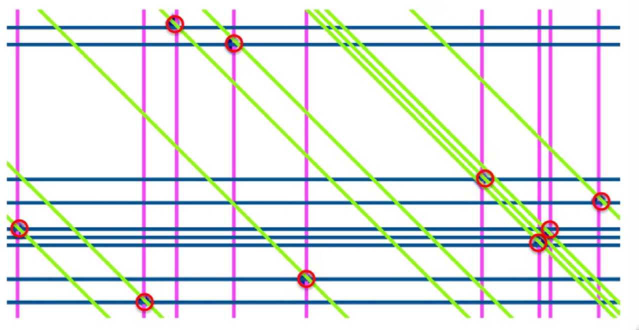

Fig. 9. A frame of an assembled multi-hit event from overlaying nine single-point measured events. Here the X, Y and U strips detecting a hit are represented by the purple, blue and green lines, respectively. Only when also using the U coordinate the red circle marked event positions can be obtained.

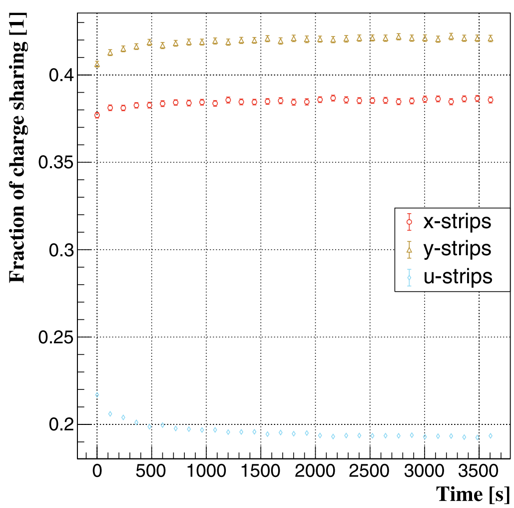

Fig. 10. Relative charge sharing between the three coordinates, after normalization to the effective detector gain.

beam, with a setup having a full triggering and tracking capability, including three triple-GEM tracking detectors with XY readout, and three scintillators for additional timing information.

Based on the experience acquired with the prototype, a redesign of the geometry of strips and insulating layers could be envisaged to get closer to the desirable equal sharing of charge between the three coordinates; the strip pitch on the U projection should also be increased to the standard 400 μm to provide a more uniform response.

A detector with more advanced design can enhance the use of the projective readout, with round GEM[3] electrodes and three sets of readout strips at 120° to each other, to have the projections symmetrically distributed. Named New EXtraordinary Tracker (NEXT), the concept is shown in Fig. 11.

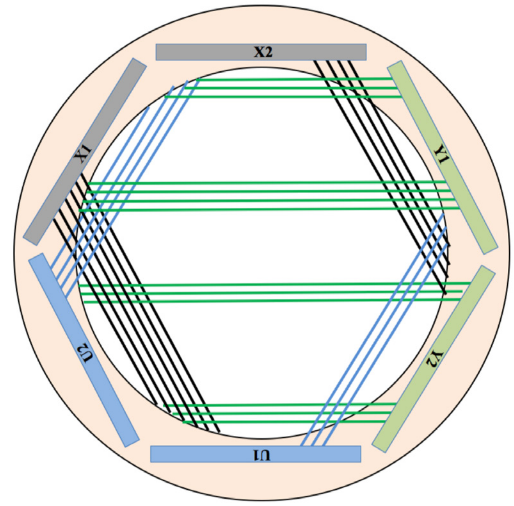

Fig. 11. A proposed NEXT circular GEM with three symmetric sets of readout strips at 120° to each other.

CRediT authorship contribution statement

K.J. Flöthner: Data curation, Formal analysis, Investigation, Methodology, Writing – original draft, Software. **D. Janssens:** Formal analysis, Investigation, Methodology, Writing – original draft, Software. **F. Brunbauer:** Writing – review & editing. **S. Ferry:** Methodology, Resources, Writing – original draft. **M. Lisowska:** Writing – review & editing. **H. Muller:** Writing – review & editing. **R. de Oliveira:** Methodology, Resources, Writing – original draft. **E. Oliveri:** Supervision, Writing – review & editing. **G. Orlandini:** Writing – review & editing. **D. Pfeiffer:** Firmware, Software, Writing – review & editing. **J. Samarati:** Writing – review & editing. **L. Ropelewski:** Project administration, Supervision, Writing – review & editing. **F. Sauli:** Conceptualization, Writing – original draft, Supervision. **L. Scharenberg:** Formal analysis, Writing – review & editing. **M. van Stenis:** Resources, Writing – review & editing. **A. Utrobicic:** Writing – review & editing. **R. Veenhof:** Writing – review & editing.

Declaration of competing interest

The authors declare that they have no known competing financial interests or personal relationships that could have appeared to influence the work reported in this paper.

Data availability

Data will be made available on request.

Acknowledgments

This work has been sponsored by the Wolfgang Gentner Programme of the German Federal Ministry of Education and Research (grant no. 13E18CHA). The work has been performed in the context of the CERN Strategic Programme on Technologies for Future Experiments. https://ep-rnd.web.cern.ch/.

[3] Minimizes distortions caused by corners which result in the warping of stretched foils.

References

[1] F. Sauli, GEM: A new concept for electron amplification in gas detectors, Nucl. Instrum. Methods Phys. Res. A 386 (1997) 531–534.

[2] J. Benlloch, A. Bressan, M. Capeáns, et al., Further developments and beam tests of the gas electron multiplier (GEM), Nucl. Instrum. Methods Phys. Res. A 419 (1998) 410–417.

[3] A. Bressan, R.D. Oliveira, A. Gandi, et al., Two-dimensional readout of GEM detectors, Nucl. Instrum. Methods Phys. Res. A 425 (1999) 254–261.

[4] F. Sauli, The gas electron multiplier (GEM): Operating principles and applications, Nucl. Instrum. Methods Phys. Res. A 805 (2016) 2–24.
[5] G. Baum, et al., The COMPASS RICH project, Nucl. Instrum. Methods Phys. Res. A 433 (1) (1999) 207–211.
[6] P. Abbon, C. Adolph, R. Akhunzyanov, et al., The COMPASS setup for physics with hadron beams, Nucl. Instrum. Methods Phys. Res. A 779 (2015) 69–115.
[7] S. Bachmann, S. Kappler, B. Ketzer, et al., High rate X-ray imaging using multi-GEM detectors with a novel readout design, Nucl. Instrum. Methods Phys. Res. A 478 (2002) 104–108.
[8] F. Sauli, Novel cherenkov photon detectors, Nucl. Instrum. Methods Phys. Res. A 553 (2005) 18–24.
[9] M. Byszewski, J. Wotschack, Resistive-strips micromegas detectors with two-dimensional readout, J. Instrum. 7 (2012) C02060.
[10] C. Altunbas, M. Capéans, K. Dehmelt, et al., Construction, test and commissioning of the triple-gem tracking detector for compass, Nucl. Instrum. Methods Phys. Res. A 490 (2002) 177–203.
[11] Garfield++, 2022, available at https://gitlab.cern.ch/garfield/garfieldpp (accessed on September 25th, 2022).
[12] COMSOL multiphysics®, 2022, available at https://www.comsol.com (accessed on September 25th, 2022).
[13] T. Alexopoulos, J. Burnens, R.D. Oliveira, et al., A spark-resistant bulk-micromegas chamber for high-rate applications, Nucl. Instrum. Methods Phys. Res. A 640 (2011) 110–118.
[14] L. Scharenberg, J. Bortfeldt, F. Brunbauer, et al., X-ray imaging with gaseous detectors using the VMM3a and the SRS, Nucl. Instrum. Methods Phys. Res. A 1011 (2021) 165576.